Shake-off measurements of electron-ion-scattering phase shifts

J. G. Story and W. E. Cooke

Department of Physics, University of Southern California, Los Angeles, California 90089-0484

(Received 7 December 1988)

Continuum electrons are produced in a specific l state with high-energy resolution using shake-off photoionization. This process is well characterized, so that the photoionization signal is an accurate measurement of the difference between the continuum electron's wave-function phase and that produced by a hydrogenic interaction. Measurements are reported showing the phase of a $Ba^+ + e^-$ in a d wave, in cases where it is well behaved, and in cases where doubly excited resonances produce rapid phase variations.

INTRODUCTION

The absolute phase of an electronic wave function is arbitrary, and thus unmeasureable; however, much can be learned about electronic interactions by studying the variations of this phase, either as a function of spatial coordinates or of energy. For example, elastic electron-scattering experiments measure how the electronic wave-function phase changes between ingoing and outgoing components. Specifically, one envisions a decomposition of an ingoing plane-wave into a linear combination of ingoing spherical waves, so that any interaction which shifts the phase of one component relative to the others will distort the balance. In that case, the outgoing combination will no longer be a plane wave, and the scattered electrons will show angular deflections. This process works best when most of the spherical components are not affected, so that one only measures the low-l phase shifts. If many of the spherical waves are phase shifted, as by a long-range interaction, the process of determining any particular phase shift becomes more complicated. Thus, for example, elastic electron-ion scattering is difficult, since the powerful (but uninteresting) Coulomb force produces considerable scattering which will obscure any other internal effects.[1,2]

Here, we report a new method of accurately measuring the phase shift of a continuum electron's wave function in the presence of an ion scatterer. The technique gains its accuracy by actually measuring how the phase shift differs from that caused by a pure Coulomb potential. Since this method uses a laser technique to produce the continuum electrons, it has an extremely high-energy resolution (better than 0.1 meV). Its major benefit, however, is that only one l-value wave is ever produced, so that no mathematical partial-wave decomposition is necessary and subtle effects should be that much more detectable. For example, this technique can be applied just as easily to cases with high l values, and in fact all of the data reported here involve $l = 2$ states. We demonstrate the technique by examining two distinct cases, one where the continuum phase has no energy dependence and a second case where autoionizing resonances introduce dramatic variations.

THEORY

When an electron is bound to an ionic core, it is easy to determine its phase shift relative to hydrogen, since the long-range behavior of the regular and irregular Coulomb wave functions require that the electron's binding energy be related to that phase shift by

$$W = -\frac{1}{2(n-\delta)^2} = -\frac{1}{2(n^*)^2} , \qquad (1)$$

where n is an integer (the principal quantum number), n^* is the effective quantum number, and δ is the quantum defect. The phase shift of the wave function relative to hydrogen is $\tau = \pi n^*$. The quantum defect thus measures what linear combination of regular and irregular Coulomb wave functions best describes the long-range behavior of the electron, and Eq. (1) results from requiring that the exponentially growing parts of these two components cancel each other.[3,4] The energy of a bound state thus produces the most accurate measurement of the electronic wave-function phase. However, continuum waves do not satisfy Eq. (1) since both the regular and irregular solutions oscillate at large distances so that neither has an exponentially growing part. Accordingly, their energy alone gives no information about the wave-function phase.

This accurate bound-state phase information can be transferred to the continuum by shaking off the bound electron as the result of an isolated core excitation (ICE) of an inner electron. The ICE technique has been developed extensively and used to excite doubly excited states of alkaline-earth atoms.[5,6] The basic idea is to put one electron into a Rydberg state, thereby isolating the other valence electron as the "core." Next, this core electron is excited while the outer, Rydberg electron is relatively undisturbed; it does not change its orbital angular momentum l, but it does change its energy to absorb (or emit) the difference between the excitation energy of the core electron and the energy of the absorbed photon. The size of the transition moment varies with energy because of two energy-dependent factors

$$T = \mu_{ge} \langle nl | n'l \rangle A_{en'l} , \qquad (2)$$

where the constant μ_{ge} is the transition moment that would be observed in the $\langle g| \rightarrow |e\rangle$ transition of the bare ion. The energy-dependent factors are $\langle nl|n'l\rangle$, the projection of the initial Rydberg electron's wave function onto its final state, and $A_{en'l}$, the amplitude of admixture of the doubly excited configuration. Thus, $|A_{en'l}|^2$ is proportional to the energy density of doubly excited states. The overlap factor itself only depends on the phase difference and energy difference between the initial and final Rydberg states[7]

$$\langle nl|n'l\rangle = \frac{\sin(\tau - \tau')}{W_{n'l} - W_{nl}} \ . \tag{3}$$

If the transition is to the bound character of the final state, as in most of the measurements performed using ICE, then the phase difference itself is related directly to the energy difference by Eq. (1). Sandner et al.[8] have been able to make very accurate measurements of the initial state's n^* by measuring the wavelengths where the zeros occur in an ICE spectrum, and then fitting them to Eq. (3). If the transition is to the continuum character of the final state, however, the phase no longer depends on the energy through Eq. (1). But in this case, the transition moment of Eq. (2) can be written in a particularly simple form which makes the dependence on the continuum electron's phase-shift explicit. First, since the outer electron will be energetically above all normal bound-state resonances, the $A_{en'l}$ coefficient becomes a constant (equal to 1 if there are no degeneracies complicating things). Then, the energy difference can be replaced with the difference between the ionic transition frequency (ω_i) and the photon frequency, so that we obtain

$$T \propto \frac{\sin(\tau - \tau')}{\hbar\omega - \hbar\omega_i} \ . \tag{4}$$

In the simplest case, the continuum phase τ' will have a constant value, and Eq. (4) will result in a photoionization cross-section that monotonically decreases as the energy denominator increases. However, if τ' has an energy dependence itself, this will show up as additional structure. The most dramatic example of such structure occurs when the continuum is coupled to an additional resonance. Then, the continuum phase will increase by a total of π over the linewidth of the resonance.

The actual measurements are somewhat more complicated, due to several effects. Degeneracies are hard to avoid. In some cases, more than one total angular-momentum value J is excited. In some cases, there are degeneracies possible even with only one J excited. Also, it is not always true that the only transition moment arises from the shake-off process. For some cases reported here, there will be two contributions, one due to shake off, and one due to shake down, producing a bound outer electron and a slightly higher ionic core excitation. Finally, in the data reported here, we did not measure the total ion signal, but instead we only detected the fluorescence produced by the excited ions left behind after the shake-off electron had left. Usually, this only multiplies the signal by a constant fluorescence-efficiency factor; however, in cases where there are nearby resonances, the

fluorescence efficiency can change, affecting the observed structure. All of these effects can be properly incorporated by using multichannel quantum-defect theory (MQDT) to calculate the $A_{en'l}$ value in Eq. (2) (actually to calculate several $A_{en'l}$ and to form the proper linear combination of them), and to modify Eq. (2) by projecting out only those final ionic states that are detected. The formalism that we employ here has been developed in detail elsewhere, for using MQDT to measure branching ratios.[9]

EXPERIMENT

All of the data reported here was obtained by monitoring the fluorescence of excited ions produced in an effusive atomic beam. We used two tunable dye lasers to excite the barium atoms stepwise through the $6s6p\ ^1P_1$ state to the $6snd\ ^1D_2$ bound Rydberg state, as shown in Fig. 1. After a delay of approximately 10 ns, to eliminate scattered light from the first two lasers, a third dye laser, near the Ba^+ $6s \rightarrow 6p_j$ transition, simultaneously excited the $6s$ core electron and shook and nd Rydberg electron into a different energy state with the same l quantum number. Finally, fluorescence was collected from one of the Ba^+ $6p_j$ ionic fine-structure states for a period of approximately 10 ns, during and after the third-laser pulse.

A typical spectrum was obtained by first setting the Rydberg excitation lasers to their required wavelengths, monitoring laser-induced fluorescence in each case to maximize the population transfer. It was usually necessary to reduce the power of each of these two lasers to prevent undesired photoionization from depleting the Rydberg population. Then, with the first two lasers fixed, the monochromator was set to detect one of the two Ba^+ $6p_j \rightarrow 6s$ transitions, while the third dye laser was scanned over the region producing shake down and shake off. Since the wavelength range of the third laser was fairly large (10–20 nm), we also measured the laser's power variation over the tuning range. The signal from the monochromator was averaged using a boxcar averager in the linear-sum mode, and stored by an AT&T 6300 microcomputer for later analysis.
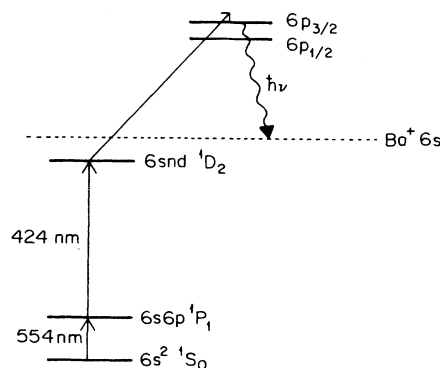

FIG. 1. Energy-level diagram of barium, showing the three-photon excitation route.

The atomic beam was produced by heating a stainless-steel oven, with a 1-mm-diam nozzle, which contains barium metal. The oven is mounted inside a caramic insulator, which is wrapped with nichrome heating wire. The entire structure is shielded by three concentric sets of stainless-steal-foil radiation shields, and enclosed inside a copper, water-cooled can. The oven can be heated to temperatures in excess of 1000 K, and produces an atomic density of approximately 4×10^{11} cm^{-3} at the interaction region, 2 cm from the nozzle. Usually, the oven was run at lower temperatures for two reasons. At very high densities, the bound-Rydberg-state population became superradiant. This produced copious broadband fluorescence which resulted in significant noise at the monitored wavelengths. Even worse, the superradiance redistributed the Rydberg population, so that the high-energy and angular-momentum resolution would be lost. The second difficulty with high atomic-beam densities was that strontium impurities would become significant. The strontium resonance line is at 461 nm, perilously close to our monitored lines. Any amplified spontaneous emission (ASE) in the third dye laser excited this resonance, again producing a background.

Above the interaction region, another water-cooled copper can traps the barium beam to prevent it from coating the optics. The interaction region is defined by the point where the atomic beam is crossed by the three collinear lasers, which pass through a series of baffles to reduce scattered light. At a right angle to both the lasers and the atomic beam, a camera lens collects the emitted fluorescence, and focuses it onto the entrance slits of a 0.1-m monochromater. All optical elements, except for a 12-cm-diam window, are kept outside the vacuum chamber; nevertheless, the camera lens can be positioned less than 10 cm from the interaction region. The monochromator is typically set for a resolution of 4 nm.

The dye lasers are pumped by the third harmonic of two independently triggerable Nd:YAG (where YAG represents yttrium aluminum garnet) lasers. The first two dye lasers are pumped by the same Nd:YAG laser, while the third dye laser is pumped by the second, delayed Nd:YAG laser. The first two lasers are simple, transversely pumped oscillators, which typically produce 0.3-mJ pulses of 5-ns duration, with a spectral bandwidth of 0.4 cm^{-1}, at wavelengths of 554 and 422 nm, respectively. The third laser is a commercial transversely pumped oscillator with two stages of transversely pumped amplifiers. It typically produces 7-mJ pulses in the 450–500 nm wavelength range, again with approximately 5-ns pulse times, and 0.5-cm^{-1} bandwidth. Often, we would operate this laser at lower powers, after realigning it to reduce the ASE output. As mentioned above, the ASE excited strontium to produce a background, but in some cases it was also very effective at photoionizing the barium Rydberg states.

RESULTS AND DISCUSSION

As a first illustration of the shake-off technique, we excited the Ba $6s19d \rightarrow$ Ba$^+$ $6p_{3/2} + e^-$ transition to produce d-wave electrons with energies of 0 to 50 meV.

There are no doubly excited states or shape resonances in this energy region, so it can be easily described by the simple model of Eq. (4). Figure 2 shows data from this excitation as the third dye laser was scanned over the wavelength range 458–438 nm. There are three prominent features in this data. First is the sharp peak at 21 952 cm^{-1}, which is due to laser-induced fluorescence of Ba$^+$ ions. Such ions are always present, being produced by collisional processes, and (mostly) by photoionization. (The second, smaller sharp peak is laser-induced fluorescence from the $5s9d$ $^1D_2 \rightarrow 5s5p$ $^1P_1$ state of strontium. The resonance transition in the impurity strontium is excited by ASE from the dye laser as mentioned above.) Underneath this peak is a broader peak, which is due to scattered laser light passing through the monochromator. The width of this peak is characteristic of the bandpass of the monochromator. The final structure is the shake-off signal, due to simultaneous excitation of the $6s$-core electron, while the Rydberg electron is shaken into a continuum state. Superimposed on the data is the simple model of Eq. (4). We made no attempt to measure the absolute phase in this case, since that would best be done by comparing the total ion yield below the threshold, where the phase is related to binding energy, to the total ion yield above the threshold.

In Fig. 3, we show the $6s19d \rightarrow 6p_{1/2} + e^-$ shake-off spectrum, which also shows the effects of shake down to $6p_{3/2}nd$ states with n between 11 and 14. The solid line through the data is our best visual fit using three channel MQDT including one bound channel and two continua channels. The bound channel is the $6p_{3/2}nd$ series which provides the shake-down transition moment as in Eq. (2). One of the continua is the shake-off continuum of Eq. (4), and the other provides an extra width to the bound states but is not directly excited. This second continuum is clearly needed, since the spectrum never reaches a true zero after the threshold turn on. We have found no significant improvement in the fit when we introduced an
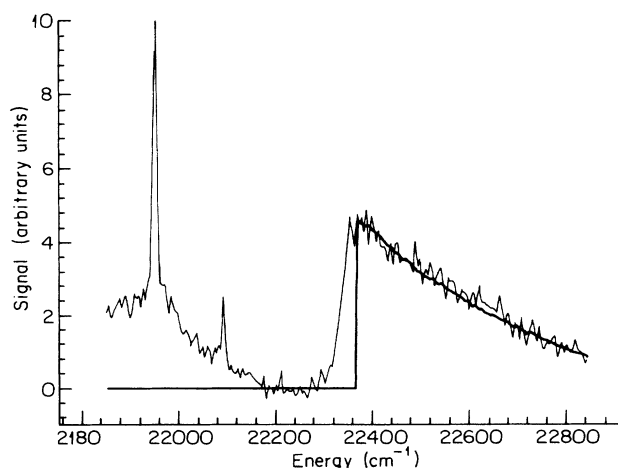

FIG. 2. Shake-off spectrum obtained from exciting the transition, Ba($6s19d$) $\rightarrow$ Ba$^+$($6p_{3/2}$) $+e^-$, by detecting the fluorescence from the excited Ba$^+$($6p_{3/2}$) ions.
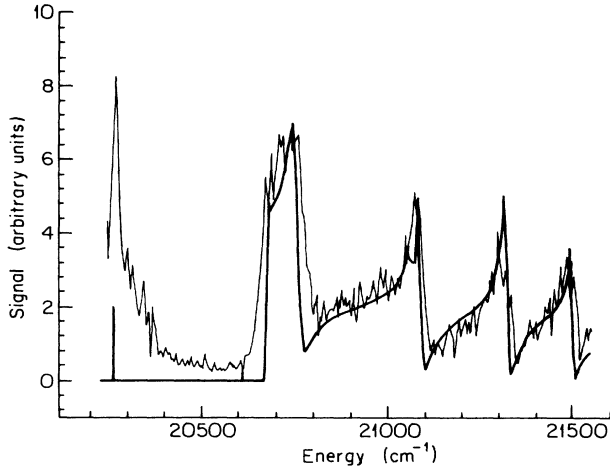
FIG. 3. Shake-off spectrum obtained from exciting the transition, $Ba(6s19d) \rightarrow Ba^+(6p_{1/2}) + e^-$, by detecting the fluorescence from the excited $Ba^+(6p_{1/2})$ ions. The resonances are $Ba(6p_{3/2}nd)$ states with $11 \leq n \leq 14$.

occur: the density of bound-state character increases, so the shake-down transition moment increases, and the shake-off continuum phase changes by π. As the phase change occurs, the shake-off transition moment changes from its near-threshold value, first increasing, then passing through zero and then returning to its initial value. Since the zero occurs at a higher energy than the resonance, the continuum phase shift must be greater than the bound resonance value. This continuum phase shift also determines where the two-transition-moment contributions, shake-down and shake-off, will be comparable. Since these two terms interfere, one expects a relatively flat region to occur when the two terms are changing at a similar rate, which means that their values are also close. Such a region can always be found, since the shake-off transition moment will decrease above threshold as $(\hbar\omega - \hbar\omega_{6p_{1/2}})^{-1}$ while the shake-down moment increases as $(\hbar\omega - \hbar\omega_{6p_{3/2}})^{-1}$, where $\omega_{6p_{1/2}}$ is the transition frequency to the lower excited core state, and $\omega_{6p_{3/2}}$ is the transition frequency to the higher excited core state. In Fig. 3, these two transition moments become approximately equal in the region between the first and second resonances.

additional continuum, whether it be detected or not. Moreover, we have found no evidence of additional bound resonances, although the $6p_{3/2}ns$ series should be present and located approximately centered between the obvious $6p_{3/2}nd$ resonances.

The MQDT fitting parameters are given in Table I. We have used a shifted R-matrix representation, so that each channel has a quantum defect and each pair of channels has a coupling represented by an off-diagonal matrix element of R.[10] This shake-off spectrum gives no information about the interactions between the continua, nor about the phase of the second continuum (which is not directly excited). The spectrum is, however, rather sensitive to four remaining MQDT parameters in this three-channel fit. The most sensitive parameter is the quantum defect of the bound $6p_{3/2}nd$ channel which determines the location of the high-energy resonances, where shake down totally dominates the spectrum. The next most sensitive parameter is the phase shift of the shake-off continuum, which determines the size of the signal just before the first $6p_{3/2}13d$ state. At threshold, before the resonance, the transition moment is dominated by just the shake-off contribution, so the ionization rate is a measure of the phase difference between the initial bound state and the shake-off continuum as in the previous example. But, near that first resonance, two things

Both of these characterizations of the continuum phase shift are only measures relative to the size of the shake-down transition moment. This moment depends (through the size of the A_{6pnd} coefficient) on the width of these resonances which in turn is determined by the sum of the squares of the two off-diagonal R-matrix elements. The way that this width is distributed between the two continua can be determined from the depth of the minima between the $6p_{3/2}nd$ resonances, particularly the first minimum. If there were no second continua, then there would always be at least one true zero between the resonances as the shake-off and shake-down transition moments canceled each other out. Even if only one term contributed, each of the two-transition moments pass through zero individually as they change sign near the resonances. The additional continuum introduces an additional solution composed of a linear combination of the two continua which is not coupled to the $6p_{3/2}nd$ resonances. Since this solution has a component of the first continua, there is a shake-off transition moment to excite it, but since it is not coupled to the resonances, the solution's phase does not change, so it provides a slowly decreasing background. The ratio of the resonant portion of the spectrum to the nonresonant portion determines the relative size of the couplings to the two continua. The sign of the coupling between the resonances and the first continua can also be determined from this spectrum. Since the sign of the A_{6pnd} coefficient depends on the sign of this coupling, and the shake-off and shake-down transition moments interfere, the sign of the coupling, and the continuum's quantum defect will determine the asymmetry of the resonant structure. There is no way to determine the sign of the coupling to the other continuum from this spectrum.

This three-channel model for this spectrum is not complete for several reasons. First, the spectrum is composed of $J = 1$ and $J = 3$ states, in a 2:3 ratio. Furthermore, al-

TABLE I. MQDT parameters for the $6s19d \rightarrow 6p_{1/2} + e^-$ spectrum shown in Fig. 3. The labels b, c_1, and c_2 correspond to the shake-down resonances, the shake-off continuum, and all other continua, respectively.

	b	c_1	c_2	δ
b	0	-0.23	-0.27	2.75
c_1		0	0	2.89
c_2			0	

though only one shake-off continuum is available for each J value, there are two $6p_{3/2}nd$ resonances. Finally, there are many continua available for each J that are not shake-off continua. Nevertheless, since the main characteristics of the spectra are well modeled, we may conclude that the quantum defects and channel couplings are not strongly J dependent. Combining the many additional continua into one should have little effect since the only role of the additional continuum in the model was to provide a nonresonant shake-off background, and additional width to the $6p_{3/2}nd$ resonances. To introduce other continua, the only necessary restriction is that the total off-diagonal R-matrix elements should sum in quadrature to the value in Table I.

CONCLUSION

This work has demonstrated that the shake-off spectrum, which results from the simultaneous excitation of a core electron and ejection of a Rydberg electron, provides a sensitive measure of the phase of the shaken-off continuum electron. This phase varies rapidly at energies near a doubly excited resonance, and this variation can result in an accurate measurement of the magnitude of individual MQDT parameters. In cases where shake-down and shake-off can both occur, the shape of the spectrum can also provide information about the sign of some of the MQDT parameters.

This technique allows a very high-resolution (0.1 MeV) determination of the phase of one particular l-value partial wave at a time. Nevertheless, there is no fundamental limitation on the specific value of l to be studied. The shake-off spectra are usually very simple with the physically measureable quantities readily discernible, a complicated partial-wave analysis is not required. Consequently, it should be an ideal technique for studies of phase variations due to subtle causes (such as shape resonances resulting from an extra potential minimum inside the core region).[11]

It is also clear that this technique can be extended to study inelastic shake off, where the transition moment is to a particular excited core-continuum wave, but a different core-continuum wave combination is detected. This should provide detailed information about one specific continuum-continuum coupling, something which is difficult to obtain from standard branching ratio measurements. Work to demonstrate this effect is currently in progress.

ACKNOWLEDGMENTS

[1]P. G. Burke and W. Eissner, in *Atoms in Astrophysics*, edited by P. G. Burke, W. B. Eissner, D. G. Hummer, and I. C. Percival (Plenum, New York, 1983), p. 1.

[2]R. J. W. Henry, Phys. Rep. **68**, 1 (1981).

[3]K. T. Lu and U. Fano, Phys. Rev. A **2**, 81 (1970).

[4]M. J. Seaton, Rep. Prog. Phys. **46**, 167 (1983).

[5]N. H. Tran, P. Pillet, R. Kachru, and T. F. Gallagher, Phys. Rev. A **29**, 2640 (1984).

[6]S. A. Bhatti and W. E. Cooke, Phys. Rev. A **28**, 756 (1983).

[7]S. A. Bhatti, C. L. Cromer, and W. E. Cooke, Phys. Rev. A **24**, 161 (1981).

[8]W. Sandner (private communication).

[9]L. D. Van Woerkom and W. E. Cooke, Phys. Rev. A **37**, 3326 (1988).

[10]W. E. Cooke and C. L. Cromer, Phys. Rev. A **32**, 2725 (1985).

[11]W. Sandner, U. Eichmann, V. Lange, and M. Völkel, J. Phys. B **19**, 51 (1986).